Published for SISSA by Springer

Received: *June 9, 2010*
Accepted: *July 12, 2010*
Published: *August 3, 2010*

Degenerate distributions in complex Langevin dynamics: one-dimensional QCD at finite chemical potential

Gert Aarts[a] **and K. Splittorff**[b]

[a] *Department of Physics, Swansea University, Swansea, U.K.*
[b] *Niels Bohr Institute, Blegdamsvej 17, DK-2100 Copenhagen Ø, Denmark*

E-mail: g.aarts@swan.ac.uk, split@nbi.dk

Abstract: We demonstrate analytically that complex Langevin dynamics can solve the sign problem in one-dimensional QCD in the thermodynamic limit. In particular, it is shown that the contributions from the complex and highly oscillating spectral density of the Dirac operator to the chiral condensate are taken into account correctly. We find an infinite number of classical fixed points of the Langevin flow in the thermodynamic limit. The correct solution originates from a continuum of degenerate distributions in the complexified space.

Keywords: Lattice QCD, Lattice Quantum Field Theory

ArXiv ePrint: 1006.0332

© SISSA 2010

doi:10.1007/JHEP08(2010)017

JHEP08(2010)017

Contents

JHEP08(2010)017

1 Introduction

Random matrix theory and chiral perturbation theory have given deep insight into one of the most persisting problems of high energy physics, namely the *sign problem*. The sign problem prohibits direct nonperturbative numerical simulations of strongly interacting matter with more quarks than antiquarks, since the measure on which the Monte Carlo method in lattice QCD seeks to sample the most important gauge field configurations is complex valued in the presence of a baryon chemical potential (for an excellent review see ref. [1]).

Besides explaining why the quenched approximation fails at nonzero chemical potential [2], random matrix theory and chiral perturbation theory have yielded highly nontrivial exact results for unquenched QCD at nonzero chemical potential μ [3, 4]. From the viewpoint of the spectrum of the Dirac operator the effect of the chemical potential is always dramatic: The chemical potential breaks the antihermiticity of the Dirac operator. This drives the eigenvalues off the imaginary axis and makes the fermion determinant complex. In contrast, one of the few facts known about QCD at nonzero chemical potential is that the chemical potential has very little effect for low temperatures as long as μ is less than the scale set by the nucleon mass. This apparent mismatch between the strong effect of μ in the fermion determinant and the small effect of μ in the gauge averaged fermion determinant (the partition function) has been coined the Silver Blaze problem [5]. The exact solutions for the unquenched average density of eigenvalues from random matrix theory and chiral perturbation theory show how this paradox is resolved [6, 7]: as the quark mass enters the band of eigenvalues in the complex plane, the average spectral density becomes complex valued and highly oscillatory. Since the period of the oscillations is inversely proportional to the space-time volume and the amplitude is exponentially large in the volume, the oscillations dramatically affect quantities such as the chiral condensate. In fact, the oscillations of the eigenvalue density are responsible for the discontinuity of the chiral condensate in the chiral limit, in strong contrast to the Banks-Casher relation valid for $\mu = 0$ [8].

The standard methods [9–26] used to evade the sign problem in QCD (reweighting, Taylor series, analytic continuation, canonical ensemble, density of states) all become extremely hard to handle numerically when the sign problem is severe, i.e. when the cancellations due to the complexity of the weight change the partition function by a factor which is exponentially large in the volume. In order to understand the range of applicability, it has proven useful to study the interplay between the sign and Silver Blaze problems. One lesson that has emerged is the importance of the phase boundary of phase quenched QCD, i.e. the theory where the complex Dirac determinant is replaced by its absolute value, for simulations of full QCD at nonzero chemical potential [27, 28].

Complex Langevin dynamics [29–32] differs from the approaches mentioned above in that importance sampling is not used. Instead the field space is complexified, which literally opens up new directions to evade the sign problem. Recently it has been shown that complex Langevin dynamics can solve the sign and Silver Blaze problems in the case of the relativistic Bose gas, i.e., a weakly coupled self-interacting complex scalar field at nonzero chemical potential, in four dimensions [33, 34]. Even though the sign problem is severe, the phase boundary of the corresponding phase quenched theory poses no obstacle. Promising results have also been obtained in heavy dense QCD and related models [35].[1]

Complex Langevin dynamics is not without its problems, though. It has been known for a long time that instabilities and runaway solutions can result in a lack of convergence of the Langevin trajectories, which necessitates in some cases the use of an adaptive stepsize [38, 39]. Recently, it was shown how a straightforward implementation of an adaptive stepsize completely eliminates instabilities in heavy dense QCD and the three-dimensional XY model at nonzero chemical potential [48]. Even when instabilities are under control, it is known that the dynamics can convergence to the wrong result [39]. This problem has recently been studied in some detail in the case of simple models with complex noise [49] and in the case of the three-dimensional XY model at nonzero chemical potential with real noise [50]. Importantly, the conclusion reached in the latter work is that the erroneous convergence is independent of the strength of the sign problem.

In this paper we test the abilities of complex Langevin dynamics against the insights obtained about the Dirac spectrum and the sign problem: For QCD in one dimension we show that complex Langevin dynamics evaluates correctly the contributions from the extreme oscillations of the eigenvalue density of the Dirac operator. This provides further evidence that complex Langevin dynamics can solve the sign problem, and that the difficulties encountered in refs. [49, 50] are not intrinsically related to sign problem but have a different origin. This clearly distinguishes this approach from the standard ones mentioned above.

One-dimensional QCD with $U(N_c)$ as gauge group contains many of the features which characterize the sign and Silver Blaze problems in four-dimensional QCD at low temperature [51].[2] Moreover, it is exactly solvable, which makes it an excellent testground for new ideas [51–56]. In ref. [51] it was shown that the spectrum of the Dirac operator in one-dimensional QCD at nonzero chemical potential is located on an ellipse in the com-

[1] Early studies of complex Langevin dynamics can be found in, e.g., refs. [36–41]. ref. [42] contains a further guide to the literature. Other recent work includes refs. [43–47].

[2] On the other hand, for $SU(N_c)$ the sign problem is not severe in one dimension [51].

JHEP08(2010)017

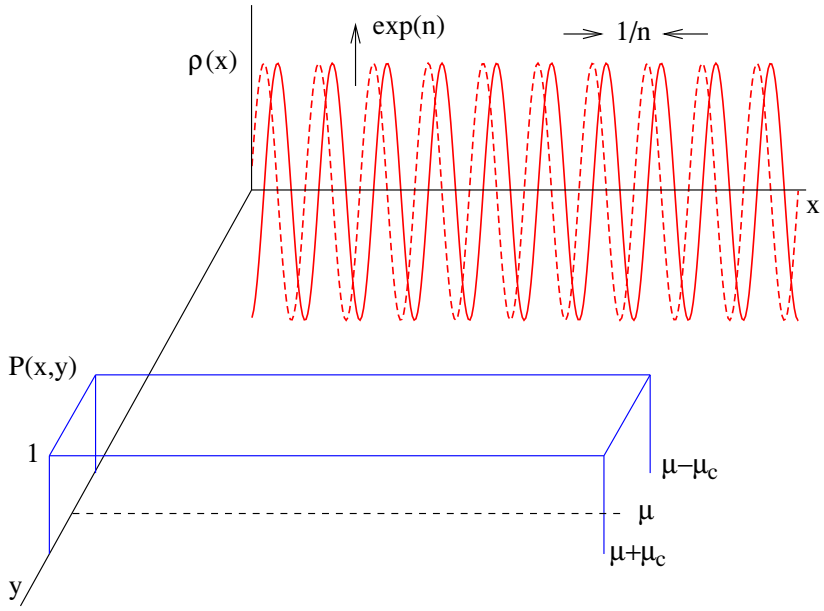

Figure 1. Sketch of how complex Langevin dynamics evades the sign problem in one-dimensional QCD, in the thermodynamic limit $n \to \infty$. The oscillatory lines at $y = 0$ represent the real (full) and imaginary (dashed) parts of the original complex weight $\rho(x)$. The uniform distribution $P(x, y) = 1$ when $\mu - |\mu_c| < y < \mu + |\mu_c|$ and 0 elsewhere represents the distribution sampled by complex Langevin dynamics. All y values in this region are equivalent, giving rise to the degeneracy mentioned in the title. The original sign problem is severe (mild) when $|\mu| > |\mu_c|$ ($|\mu| < |\mu_c|$).

plex plane. Since the chiral condensate can be viewed as the electric field originating from charges located at the positions of the eigenvalues, one would naively conclude that the chiral condensate is zero when the quark mass is inside the ellipse. However, the unquenched eigenvalue density on this ellipse is complex and rapidly oscillating: the correct chiral condensate, with a discontinuity when the quark mass goes through zero, emerges only when all highly oscillatory complex contributions are taken into account properly. Even though the Dirac spectrum in four-dimensional QCD is spread out into a band, it is exactly the same structure of the oscillations which is responsible for chiral symmetry breaking [6, 7].

In this paper we establish a first link between the complex oscillations of the spectral density of the Dirac operator and complex Langevin dynamics, and demonstrate that the sign and Silver Blaze problems in one dimensional QCD are solved by complex Langevin dynamics. We encounter a number of surprises not seen before. Most importantly, we find that complex Langevin trajectories depend on the initial conditions, even in the limit of infinite Langevin time: the dynamics is not ergodic. Nevertheless, all trajectories yield equivalent results, resulting in a degenerate set of stationary distributions in the complexified space. In the thermodynamic limit, this continuum of distributions becomes particularly simple and is sketched in figure 1. Moreover, it is known that classical fixed points can play an important role in localizing the dynamics in the complexified field space. In most models accessible to an analytical study, only a handful of fixed points exists. Instead, in the case studied here, we find an infinite number of stable and unstable classical fixed

JHEP08(2010)017

points in the thermodynamic limit. As in ref. [57] where the factorization method was tested with random matrix results, our results demonstrate the usefulness of exact results as benchmarks for numerical methods which seek to deal with the sign problem.

The paper is organized as follows. After a brief review of the relevant analytic results in one-dimensional QCD in section 2, we set up and study the complex Langevin dynamics problem in section 3. In section 4 we show that one stationary distribution of the corresponding Fokker-Planck equation can be found analytically for all n, but that, surprisingly, this distribution is not realized in the actual dynamics. This is explained in terms of classical flow and fixed points in section 5, where a larger set of solutions to the Fokker-Planck equation in the thermodynamic limit is given. It is demonstrated analytically that this continuum of degenerate distributions yields the correct result for the chiral condensate. Section 6 contains a brief summary and outlook.

2 One-dimensional QCD and the sign problem

We follow closely refs. [51, 54] and consider QCD with gauge group $\mathrm{U(N_c)}$ in one dimension on a lattice with n points. Here n is assumed even throughout and is taken to infinity in the thermodynamic limit. The (staggered) fermions obey antiperiodic boundary conditions and chemical potential is introduced as usual [58]. We choose the gauge where all link variables are equal to unity, except at the final timeslice. The one flavour fermion determinant can then be written as

$$\det[D(U)+m] = \det[e^{n\mu_c} + e^{-n\mu_c} + e^{n\mu}U + e^{-n\mu}U^\dagger], \tag{2.1}$$

where U is the remaining link variable and μ_c is related to the fermion mass m via

$$m = \sinh \mu_c. \tag{2.2}$$

Since there is no Yang-Mills action in one dimension, the partition function has the simple form

$$Z = \int_{\mathrm{U(N_c)}} dU \, \det[D(U)+m] = \frac{\sinh[n\mu_c(N_c+1)]}{\sinh(n\mu_c)}. \tag{2.3}$$

One possible way to implement complex Langevin dynamics for this class of theories is to evaluate the remaining group integral over the final link variable using complex Langevin dynamics. Such an approach has been explored in ref. [35] in the case of SU(3) and excellent agreement with exact results has been obtained. Here we wish to make a connection between Langevin dynamics on one hand and properties of the Dirac spectrum on the other hand. For that reason we take a different route and first cast the chiral condensate as an integral over the eigenvalue density of the Dirac operator. The resulting integral is subsequently solved with complex Langevin dynamics.

The partition function is independent of the chemical potential. On the contrary, the eigenvalues of the Dirac operator $D(U)$,

$$\lambda_{k,l} = \frac{1}{2}\left(e^{\frac{2\pi i(k+1/2)+i\theta_l}{n}+\mu} - e^{-\frac{2\pi i(k+1/2)+i\theta_l}{n}-\mu}\right), \tag{2.4}$$

JHEP08(2010)017

depend on the chemical potential. Here $k = 1, \ldots, n$, and $\exp(i\theta_l)$ with $l = 1, \ldots, N_c$, are the eigenvalues of U. The eigenvalues lie on an ellipse in the complex plane,

$$\left(\frac{\mathrm{Re}\,\lambda_{k,l}}{\sinh(\mu)}\right)^2 + \left(\frac{\mathrm{Im}\,\lambda_{k,l}}{\cosh(\mu)}\right)^2 = 1. \tag{2.5}$$

Consequently, the eigenvalue density,

$$\rho(z;\mu) = \frac{1}{Z}\int_{\mathrm{U(N_c)}} dU\ \det[D(U)+m]\ \sum_{k,l}\delta^2(z-\lambda_{k,l}), \tag{2.6}$$

depends on μ. The chiral condensate (normalized with the one-dimensional volume),

$$\begin{aligned}\Sigma &= \frac{1}{n}\frac{\partial}{\partial m}\log Z \\ &= \frac{1}{\cosh(\mu_c)}\left[(1+N_c)\coth\left[(1+N_c)\,n\mu_c\right] - \coth\left(n\mu_c\right)\right],\end{aligned} \tag{2.7}$$

is, however, independent of μ since the partition function is. Expressing the chiral condensate as an integral over the μ-dependent eigenvalue density,

$$\Sigma = \int d^2z\,\frac{\rho(z;\mu)}{z+m}, \tag{2.8}$$

the μ-independence of Σ is far from obvious. We note that the condensate Σ can be viewed as the electric field created by the charge density $\rho(z;\mu)$. Naively one would therefore expect the condensate to be zero when the mass m is inside the ellipse in the complex plane, i.e. when $|m| < |\sinh(\mu)|$ or equivalently $|\mu_c| < |\mu|$. However, this is in contradiction with the known μ-independence of the condensate. This is the *Silver Blaze problem* in one-dimensional QCD: it illustrates the severe problems encountered when lattice QCD is applied for nonzero values of the chemical potential. It is thus of practical interest to understand if complex Langevin dynamics is able to reproduce this μ-independence.

In one dimension the essential properties of the eigenvalue density do not depend on N_c. For all N_c the eigenvalues lie on an ellipse in the complex plane and the eigenvalue density is a rapidly oscillating complex function with a diverging amplitude in the thermodynamic limit (when $|\mu| > |\mu_c|$). We continue therefore now with the case $N_c = 1$, for which the spectral density has a simple analytical form [51]. If the ellipse is parametrized by an angle α, i.e.,

$$z = \frac{1}{2}\left(e^{i\alpha+\mu} - e^{-i\alpha-\mu}\right), \tag{2.9}$$

the eigenvalue density becomes [51], up to an overall constant which cancels in eq. (2.11) below,

$$\rho(\alpha;\mu) = 1 - \frac{\cosh[n(\mu+i\alpha)]}{\cosh(n\mu_c)}. \tag{2.10}$$

Observe that the eigenvalue density is complex and is highly oscillating when $|\mu| > |\mu_c|$, as illustrated in figure 1. The chiral condensate is then written as

$$\Sigma = \int_0^{2\pi}\frac{d\alpha}{2\pi}\,\rho(\alpha;\mu)\Sigma(\alpha;\mu), \tag{2.11}$$

JHEP08(2010)017

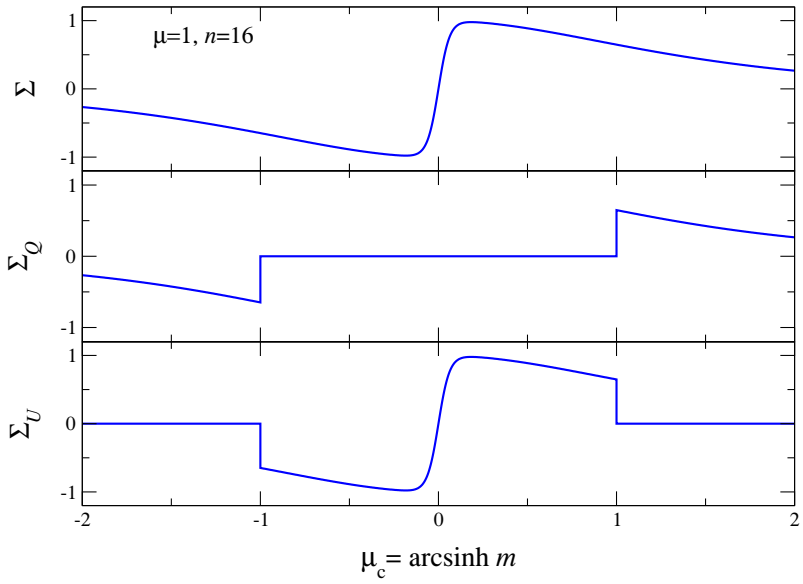

Figure 2. The full μ-independent chiral condensate (top) in one-dimensional QCD along with the contributions from the constant (middle) and oscillating part (bottom) of the eigenvalue density. As in four-dimensional QCD, at nonzero μ the discontinuity of the chiral condensate at zero quark mass in the thermodynamic limit is entirely due to the complex oscillating part of the eigenvalue density (compare to figure 2 of ref. [59]).

with

$$\Sigma(\alpha;\mu) = \frac{1}{\sinh(\mu + i\alpha) + \sinh(\mu_c)}, \tag{2.12}$$

and is evaluated as

$$\Sigma = \frac{\tanh(n\mu_c)}{\cosh(\mu_c)}, \tag{2.13}$$

in agreement with eq. (2.7) for $N_c = 1$. In the thermodynamic limit the discontinuity when μ_c goes through zero appears and

$$\lim_{n\to\infty} \Sigma = \frac{\mathrm{sgn}(\mu_c)}{\cosh(\mu_c)}. \tag{2.14}$$

As was first observed in the microscopic limit of four-dimensional QCD [6, 7], the strong complex oscillations of the eigenvalue density are responsible for the discontinuity of the chiral condensate at zero quark mass in the thermodynamic limit. To see this it is advantageous to split the contribution to the chiral condensate into the contribution from the smooth part of the density (the "1"),

$$\Sigma_Q = \int_0^{2\pi} \frac{d\alpha}{2\pi}\, \Sigma(\alpha;\mu) = \Theta\left(|\mu_c| - |\mu|\right) \frac{\mathrm{sgn}(\mu_c)}{\cosh(\mu_c)}, \tag{2.15}$$

and the contribution from the complex oscillating part,

$$\Sigma_U = \int_0^{2\pi} \frac{d\alpha}{2\pi}\, \left[\rho(\alpha;\mu) - 1\right] \Sigma(\alpha;\mu) = \Sigma - \Sigma_Q. \tag{2.16}$$

This is illustrated in figure 2. The smooth part contributes only for large quark mass (i.e. $|\mu_c| > |\mu|$) while the oscillating part makes up the chiral condensate when $|\mu_c| < |\mu|$. In

JHEP08(2010)017

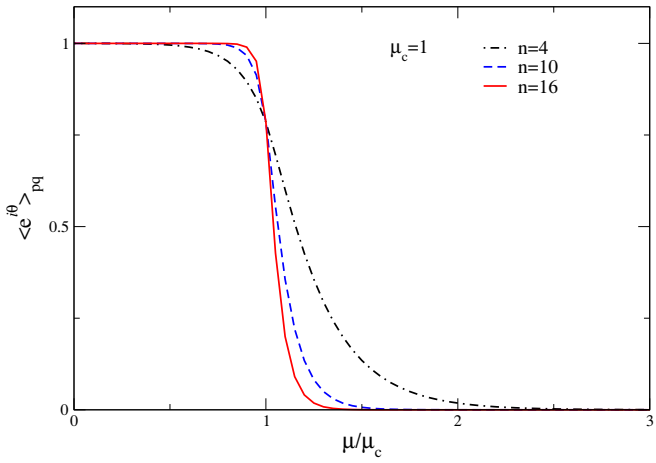

Figure 3. Expectation value of the phase factor $e^{i\theta} = \rho(\alpha;\mu)/|\rho(\alpha;\mu)|$ with respect to the phase quenched weight as a function of μ/μ_c for $\mu_c = 1$ and $n = 4, 10, 16$.

particular, the oscillations of the eigenvalue density are responsible for the discontinuity of the chiral condensate when the quark mass goes through zero and provide the solution to the Silver Blaze problem. We will demonstrate below that complex Langevin correctly evaluates the contribution from these oscillations.

3 Complex Langevin dynamics

We interpret $\rho(\alpha;\mu)$ as the complex weight, satisfying the usual relation $\rho^*(\alpha;\mu) = \rho(\alpha;-\mu^*)$, and write it as

$$\rho(\alpha;\mu) = |\rho(\alpha;\mu)|e^{i\theta}. \tag{3.1}$$

The severity of the sign problem can be assessed via the expectation value of the phase $e^{i\theta}$ with respect to the phase quenched weight. We hence define the average phase factor as

$$\langle e^{i\theta}\rangle_{\rm pq} = \frac{\int_0^{2\pi} d\alpha\, \rho(\alpha;\mu)}{\int_0^{2\pi} d\alpha\, |\rho(\alpha;\mu)|}, \tag{3.2}$$

which is shown in figure 3 for various values of n. We find the sign problem to be mild (absent) when $|\mu| < |\mu_c|$ and severe when $|\mu| > |\mu_c|$. All the dependence on μ in figure 3 emerges from the denominator in eq. (3.2), since the numerator is μ-independent. The theory with the phase quenched weight therefore has a transition at $\mu = \mu_c$: our model behaves exactly as QCD in the region where $0 \le \mu \lesssim m_B/3$, with μ_c playing the role of $m_\pi/2$.

The complex weight $\rho(\alpha;\mu)$ is a highly oscillatory complex function, with period $2\pi/n$. From its real and imaginary parts,

$$\mathrm{Re}\,\rho(\alpha;\mu) = 1 - \frac{\cosh(n\mu)}{\cosh(n\mu_c)}\cos(n\alpha), \tag{3.3a}$$

$$\mathrm{Im}\,\rho(\alpha;\mu) = \frac{\sinh(n\mu)}{\cosh(n\mu_c)}\sin(n\alpha), \tag{3.3b}$$

JHEP08(2010)017

we note that the sign problem is severe when the real part of the distribution is not positive-definite and, for large n, the amplitude of oscillations grows exponentially as $\exp[n(|\mu| - |\mu_c|)]$. On the other hand, when the sign problem is absent, the amplitude of oscillations decreases exponentially in the thermodynamic limit.

We now apply complex Langevin dynamics to study QCD in one dimension. We interpret $\rho(\alpha;\mu)$ as the distribution and

$$S(\alpha;\mu) = -\log\rho(\alpha;\mu) \tag{3.4}$$

as the complex action. We complexify the angle $\alpha \to x + iy$. The discretized Langevin equations, for general complex noise, read

$$x_{j+1} = x_j + \epsilon K_x(x_j, y_j) + \sqrt{\epsilon N_{\rm R}}\eta_j^{\rm R}, \tag{3.5a}$$

$$y_{j+1} = y_j + \epsilon K_y(x_j, y_j) + \sqrt{\epsilon N_{\rm I}}\eta_j^{\rm I}, \tag{3.5b}$$

where ϵ is the Langevin stepsize and Langevin time is $\vartheta = j\epsilon$. The drift terms are determined by

$$K_x = -{\rm Re}\,\frac{\partial S}{\partial\alpha}\Big|_{\alpha\to x+iy}, \qquad K_y = -{\rm Im}\,\frac{\partial S}{\partial\alpha}\Big|_{\alpha\to x+iy}, \tag{3.6}$$

with the classical drift term

$$\frac{\partial S}{\partial\alpha}\Big|_{\alpha\to x+iy} = in\frac{\sinh[n(\mu - y + ix)]}{\cosh(n\mu_c) - \cosh[n(\mu - y + ix)]}. \tag{3.7}$$

The noise satisfies

$$\langle\eta_j^{\rm R}\rangle = \langle\eta_j^{\rm I}\rangle = \langle\eta_j^{\rm R}\eta_{j'}^{\rm I}\rangle = 0, \quad \langle\eta_j^{\rm R}\eta_{j'}^{\rm R}\rangle = \langle\eta_j^{\rm I}\eta_{j'}^{\rm I}\rangle = 2\delta_{jj'}, \tag{3.8}$$

with $N_{\rm R} - N_{\rm I} = 1$. Finally, the Fokker-Planck equation underlying this stochastic process reads, in the limit that $\epsilon \to 0$,

$$\partial_\vartheta P(x,y;\vartheta) = \left[\partial_x\left(N_{\rm R}\partial_x - K_x\right) + \partial_y\left(N_{\rm I}\partial_y - K_y\right)\right]P(x,y;\vartheta), \tag{3.9}$$

where $P(x,y;\vartheta)$ is a distribution in the complexified space, which should be real and positive. We specialize to real noise ($N_{\rm I} = 0$) in most of the paper, but briefly come back to complex noise at the end.

We have solved the Langevin equations numerically, using a moderate stepsize of $\epsilon = 0.001$ and Langevin times up to $\vartheta = 5\times10^4$. The results for the condensate are shown in figure 4 for four values of n. We observe excellent agreement with the exact results, indicated by the lines. Note that the sign problem is severe when $-1 < \mu_c < 1$. The discontinuity at $\mu_c = 0$ emerges in the thermodynamic limit. We have done simulations for various values of μ to confirm that the condensate only depends on μ_c and not on μ.

4 One stationary distribution

In order to understand why complex Langevin dynamics has no apparent problem with the sign and Silver Blaze problems, we first note that μ can be eliminated completely from

JHEP08(2010)017

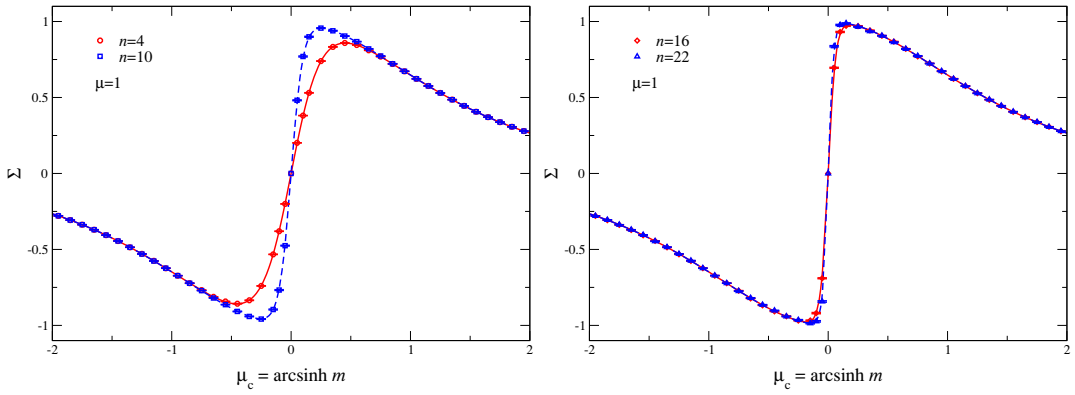

Figure 4. Condensate for $n = 4, 10$ (left) and $n = 16, 22$ (right) as a function of μ_c for fixed $\mu = 1$. The data points are obtained with complex Langevin dynamics, while the lines are the exact result (2.13).

the dynamics by writing $y = \mu + \bar{y}$, which removes μ from the classical drift term. The Silver Blaze problem is therefore trivially solved by the complexification. Taking this one step further, we specialize to the case $y = \mu$. The corresponding drift term

$$\tilde{K} \equiv -\frac{\partial S}{\partial \alpha}\Big|_{\alpha \to x + i\mu} = n \frac{\sin(nx)}{\cosh(n\mu_c) - \cos(nx)}, \tag{4.1}$$

is entirely real, such that there is no dynamics in the imaginary direction (in the case of real noise). We can then interpret the remaining Langevin evolution as a real process, shifted in the complex plane, with a force $\tilde{K}$ which can be derived from an action,

$$\tilde{S} = -\log[\cosh(n\mu_c) - \cos(nx)] + \text{constant}, \tag{4.2}$$

such that $\tilde{K} = -\partial \tilde{S}/\partial x$. It follows that the associated probability distribution can be written as[3]

$$P_\delta(x, y) = p_x(x)\delta(y - \mu), \tag{4.3}$$

with

$$p_x(x) = \exp(-\tilde{S}), \qquad \tilde{S}(x) = S(x; \mu = 0), \tag{4.4}$$

where the constant has been fixed by the normalization condition

$$\int \frac{dxdy}{2\pi} P(x, y) = 1. \tag{4.5}$$

This distribution is related to the original complex weight as

$$p_x(x) = \rho(x; \mu = 0), \tag{4.6}$$

and is real and positive.

[3]See also refs. [1, 49, 60] for similar cases.

JHEP08(2010)017

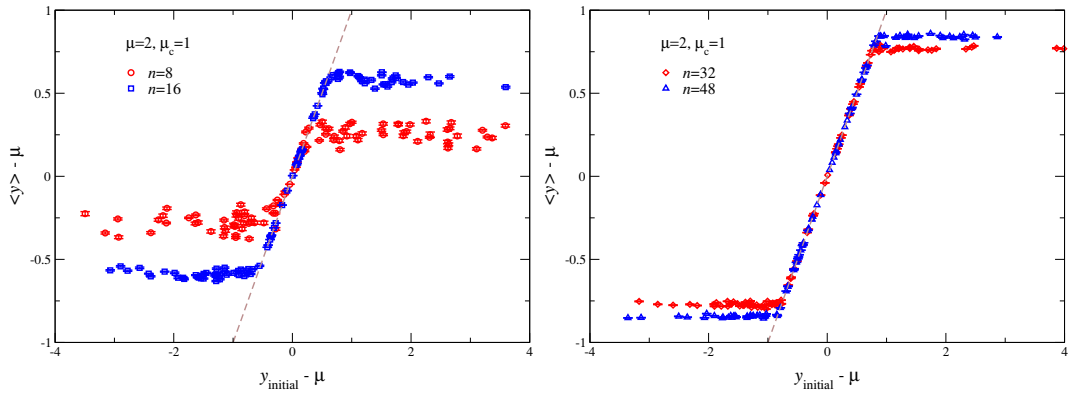

Figure 5. Expectation value $\langle y\rangle - \mu$ as a function of (random) initial condition $y_{\rm initial} - \mu$ for fixed $\mu = 2$, $\mu_c = 1$ for $n = 8, 16$ (left) and $32, 48$ (right). The dashed lines indicate $\langle y\rangle = y_{\rm initial}$.

This distribution gives the correct chiral condensate, since

$$\begin{aligned}\Sigma &= \int_0^{2\pi} \frac{dx}{2\pi} \int_{-\infty}^{\infty} dy\, P_\delta(x,y)\Sigma(x+iy;\mu) \\ &= \int_0^{2\pi} \frac{dx}{2\pi}\, p_x(x)\Sigma(x+i\mu;\mu) \\ &= \int_0^{2\pi} \frac{dx}{2\pi}\, \rho(x;0)\Sigma(x;0) = \frac{\tanh(n\mu_c)}{\cosh(\mu_c)}. \end{aligned} \tag{4.7}$$

The solution we found is indeed a stationary solution of the Fokker-Planck equation (3.9) when $N_{\rm I} = 0$, since $K_y\delta(y-\mu) = 0$ and $\tilde{K} = K_x(\mu = 0)$. To conclude, we have found a stationary distribution in the complexified space. If a trajectory is initialized at $y = \mu$, we can consider a real Langevin process for which standard arguments can be used to demonstrate that the correct stationary distribution is reached in the limit of infinite Langevin time.

Surprisingly, $P_\delta(x,y)$ is not the unique stationary distribution: trajectories initialized with $y \neq \mu$ are not in general attracted to $y = \mu$. To illustrate this, we have computed the expectation value $\langle y\rangle$ for a large number of trajectories, starting from different initial conditions $y_{\rm initial}$. The resulting $\langle y\rangle$ is shown in figure 5 as a function of $y_{\rm initial}$ for $n = 8, 16$ (left) and $n = 32, 48$ (right), using 100 initial conditions randomly distributed around $y_{\rm initial} = \mu$ for each n. Note that we have subtracted $\mu = 2$ from both $\langle y\rangle$ and $y_{\rm initial}$. If all trajectories are attracted to the stationary distribution P_δ, one should obtain $\langle y\rangle = \mu$ independent of $y_{\rm initial}$. Instead we find that the average value of y is linearly correlated with the initial value when $y_{\rm initial} - \mu$ is small and independent of the initial value when $y_{\rm initial} - \mu$ is larger and approaches $\pm\mu_c$. Despite this, all trajectories yield a value for the condensate that is consistent with the exact result.[4] The y value where the crossover between the linear dependence on and the independence of the initial condition occurs,

[4]Taking the average of the 100 initial conditions we find $\Sigma = 0.6479(2)$ for $n = 8$, $0.6483(3)$ for $n = 16$, $0.6483(4)$ for $n = 32$ and $0.6478(3)$ for $n = 48$. The exact result is $\Sigma = 0.648054$.

JHEP08(2010)017

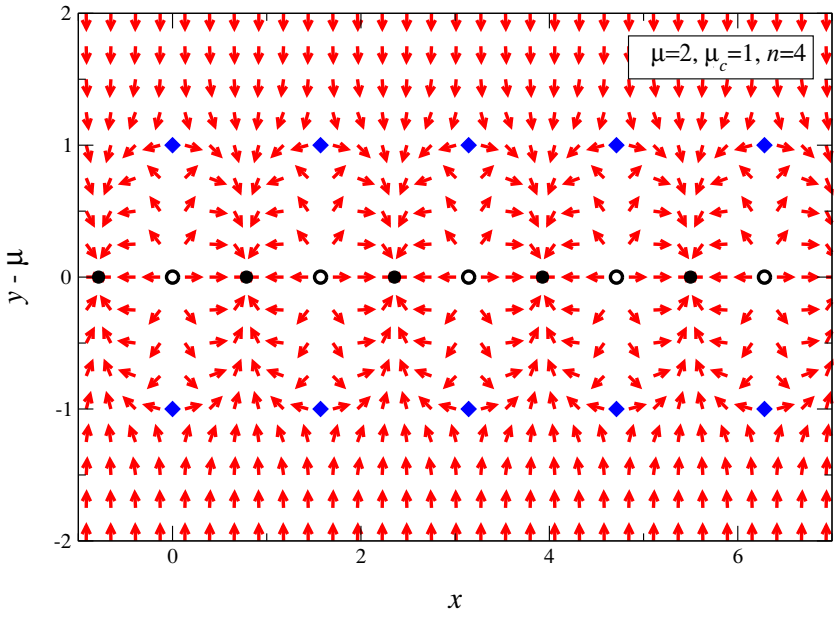

Figure 6. Flow pattern for $\mu = 2$, $\mu_c = 1$ and $n = 4$. The filled/open black dots are stable/unstable fixed points, the diamonds indicate a diverging flow. On the line $y = \mu$, $K_y = 0$. The arrows are normalized to have the same length.

depends on n. From the numerical results we infer that in the thermodynamic limit

$$\lim_{n\to\infty}\langle y\rangle = \begin{cases} \mu + |\mu_c| & \text{when } \ y_{\text{initial}} > \mu + |\mu_c|, \\ y_{\text{initial}} & \text{when } \ \mu - |\mu_c| < y_{\text{initial}} < \mu + |\mu_c|, \\ \mu - |\mu_c| & \text{when } \ y_{\text{initial}} < \mu - |\mu_c|. \end{cases} \tag{4.8}$$

We conclude that the dynamics is not ergodic. Nevertheless, the expectation values of the condensate are consistent within the error with the analytical result for all initial conditions. The stationary distribution at $y = \mu$ is only realized when $y_{\text{initial}} = \mu$.

5 Classical flow and degenerate distributions

In this section we explain the numerical results observed above. We first show analytically why the dynamics is not ergodic and subsequently demonstrate that a continuum of distributions exist in the thermodynamic limit, all yielding the correct condensate.

The nonergodicity can be understood from the classical flow. We split the force explicitly in real and imaginary parts and write

$$K_x = n\frac{AE - C}{(E - AC)^2 + B^2D^2}D, \qquad K_y = n\frac{A - CE}{(E - AC)^2 + B^2D^2}B, \tag{5.1}$$

in terms of

$$A = \cosh[n(\mu - y)], \qquad C = \cos(nx), \tag{5.2a}$$

$$B = \sinh[n(\mu - y)], \qquad D = \sin(nx), \qquad E = \cosh(n\mu_c). \tag{5.2b}$$

JHEP08(2010)017

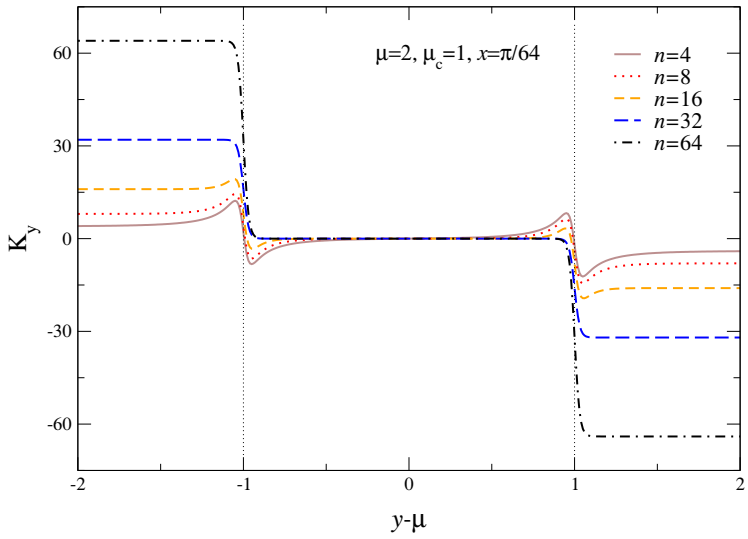

Figure 7. Force K_y in the y-direction as a function of $y-\mu$ at fixed $x=\pi/64$ for various values of n and $\mu=2$, $\mu_c=1$.

Classical fixed points are determined by $K_x=K_y=0$. We find

– n stable fixed points at

$$x=(2k+1)\pi/n,\quad y=\mu\quad (k=0,\ldots,n-1). \tag{5.3}$$

– n unstable fixed points at

$$x=2k\pi/n,\quad y=\mu\quad (k=0,\ldots,n-1). \tag{5.4}$$

– $2n$ points where the flow diverges ($K_x=0, K_y=\infty$) at

$$x=2k\pi/n,\quad y=\mu\pm\mu_c\quad (k=0,\ldots,n-1). \tag{5.5}$$

The flow patterns are shown in figure 6 for $n=4$. For larger values of n, the number of fixed points and hence the density of regions where the flow changes direction increase. The region bounded by $\mu\pm\mu_c$ is an attractor region: all trajectories will end up here, irrespective of the initial y value. The line $y=\mu$, however, is not an attractor due to the alternating stable and unstable fixed points, except when starting exactly on it. For obvious reasons, we will refer to the region bounded by $y=\mu\pm\mu_c$ as the inside region, while the two regions where $|y-\mu|>|\mu_c|$ are referred to as the outside regions.

The arrows in figure 6 are normalized to have the same length. To indicate the strength of the force in y direction, we show in figure 7 the value of K_y at fixed $x=\pi/64$. We observe that in the thermodynamic limit K_y goes to zero in the inside region, whereas its magnitude increases linearly with n in the outside region. This is confirmed by the

JHEP08(2010)017

following expressions for K_y in the thermodynamic limit,[5]

$$\lim_{n\to\infty} K_y = \begin{cases} n\,\mathrm{sgn}(y-\mu)e^{-n(|\mu_c|-|\mu-y|)}\cos(nx) \to 0, & \text{inside,} \\ n\,\mathrm{sgn}(\mu-y) \to \pm\infty, & \text{outside.} \end{cases} \tag{5.6}$$

On the other hand, the force in the x direction goes to zero both on the inside and the outside,

$$\lim_{n\to\infty} K_x = \begin{cases} ne^{-n(|\mu_c|-|\mu-y|)}\sin(nx) \to 0, & \text{inside,} \\ ne^{-n(|\mu-y|-|\mu_c|)}\sin(nx) \to 0, & \text{outside.} \end{cases} \tag{5.7}$$

This confirms that for large $|y|$ the flow is attracted to the region $\mu - |\mu_c| < y < \mu + |\mu_c|$ very efficiently. Once inside, the forces vanish exponentially, with the rate determined by the vicinity to the boundary at $\pm\mu_c$. This explains the dependence on initial conditions found in figure 5.

In the thermodynamic limit, the forces in the inside region vanish. The stochastic evolution then reduces to simple diffusion in a square well bounded by $y = \mu \pm \mu_c$ (and periodic in x). In the case of real noise the diffusion is one-dimensional. In the case of complex noise, the diffusion is two-dimensional. It is now straightforward to deduce the stationary solution of the Fokker-Planck equation in the thermodynamic limit. We find

$$\lim_{n\to\infty} P(x,y) = \begin{cases} p_y(y) & \text{when } \mu - |\mu_c| < y < \mu + |\mu_c|, \\ 0 & \text{elsewhere.} \end{cases} \tag{5.8}$$

In the case of real noise, $p_y(y)$ depends on the initial conditions as

$$p_y(y) = \begin{cases} \delta(y-\mu-|\mu_c|-\varepsilon) & \text{when } y_{\text{initial}} \geq \mu + |\mu_c|, \\ \delta(y-y_{\text{initial}}) & \text{when } \mu - |\mu_c| < y_{\text{initial}} < \mu + |\mu_c|, \\ \delta(y-\mu+|\mu_c|+\varepsilon) & \text{when } y_{\text{initial}} \leq \mu - |\mu_c|, \end{cases} \tag{5.9}$$

where $\varepsilon \downarrow 0$, see footnote 5. For complex noise, $p_y(y)$ is determined by the normalization condition as

$$p_y(y) = \frac{1}{2|\mu_c|}. \tag{5.10}$$

The resulting distribution is sketched in figure 1.

This continuous family of distributions all yields the correct value for the condensate. To demonstrate this, we write the condensate as

$$\Sigma = \int \frac{dxdy}{2\pi} P(x,y)\Sigma(x+iy;\mu) = \int dy\, p_y(y) \int \frac{dx}{2\pi}\Sigma(x+iy;\mu), \tag{5.11}$$

and evaluate the x integral by contour integration. In terms of $z = e^{ix}$, we find

$$\int \frac{dx}{2\pi}\Sigma(x+iy;\mu) = \int_{|z|=1} \frac{dz}{2\pi i} \frac{-2e^{-\mu+y}}{(z-z_1)(z-z_2)}, \tag{5.12}$$

[5] Exactly on the borderlines $y = \mu \pm \mu_c$, K_y diverges for specific values of x, see eq. (5.5). Away from these points, the force is directed inwards.

JHEP08(2010)017

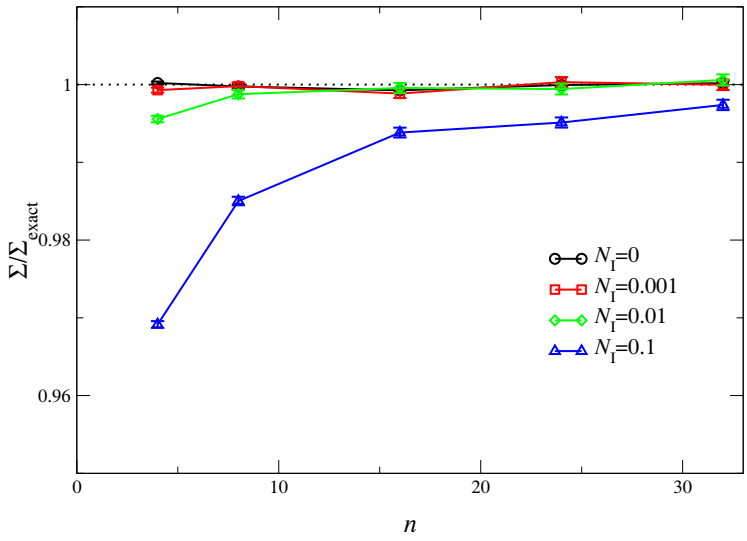

Figure 8. Normalized condensate $\Sigma/\Sigma_{\text{exact}}$ as a function of n in the case of complex noise, $N_{\text{I}} > 0$. It is seen that in this case complex noise works in the thermodynamic limit, $n \to \infty$.

with

$$z_1 = e^{\mu_c - \mu + y}, \qquad z_2 = -e^{-\mu_c - \mu + y}. \tag{5.13}$$

In the inside region, $\mu - |\mu_c| < y < \mu + |\mu_c|$, only the pole at z_2 (z_1) contributes when $\mu_c > 0$ ($\mu_c < 0$). The result is

$$\int \frac{dx}{2\pi}\, \Sigma(x + iy; \mu) = \frac{\text{sgn}(\mu_c)}{\cosh(\mu_c)}, \tag{5.14}$$

for all values of y in the inside region. The remaining integral over y in eq. (5.11) is now trivially performed and yields unity due the normalization condition. We conclude therefore that the correct result for the condensate is obtained and that the degenerate distributions are all equivalent.

It is known that complex noise does not work in general [49] and that is also what we find here for finite n. However, in this example complex noise can be expected to work in the thermodynamic limit, since in that case the dynamics takes place in a square well with infinitely-high walls at $y = \mu \pm \mu_c$. This is demonstrated in figure 8, where the condensate is shown as a function of n for various values of N_{I}.

6 Conclusion

We have established a first link between the complex oscillations of the universal microscopic spectral density of the Dirac operator and complex Langevin dynamics. For QCD in one dimension we have shown how complex Langevin dynamics correctly evaluates the chiral condensate given the complex and strongly oscillating unquenched eigenvalue density. The exact solution of the Fokker-Planck equation in the thermodynamic limit shows explicitly how the complex Langevin method can deal with the severe sign problem present.

JHEP08(2010)017

Surprisingly we did not find a unique solution but rather a continuum of degenerate solutions, which all yield the correct chiral condensate. This has been shown analytically in the thermodynamic limit and demonstrated numerically for finite systems.

The exact solution presented here offers a direct analytic indication that complex Langevin dynamics can solve the sign problem. While there exist examples where the complex Langevin method is problematic [39, 49, 50], we would like to stress that the difficulties encountered with complex Langevin dynamics are independent of the severity of the sign problem. For instance, in ref. [50] it was demonstrated that the failure of complex Langevin dynamics is caused by an apparent incorrect exploration of the complexified field space by the Langevin evolution, similar to the case of complex noise considered in ref. [49]. In the cases where the method works well, such as in refs. [33, 34] and above, the thermodynamic limit poses no obstacle. This is in strong contrast to the standard methods (reweighting, Taylor series, imaginary chemical potential and analytic continuation), which work well in small volumes but eventually break down due the sign problem in large volumes. Our findings therefore strongly encourage further studies of complex Langevin dynamics at nonzero chemical potential.

Acknowledgments

Part of this work was carried out at the Yukawa Institute for Theoretical Physics in Kyoto. It is a pleasure to thank the Yukawa Institute, and especially Kenji Fukushima, for hospitality. We thank Poul Henrik Damgaard, Philippe de Forcrand, Simon Hands, Frank James, Erhard Seiler, Ion-Olimpiu Stamatescu and Jac Verbaarschot for discussions. Finally, we are grateful to the Niels Bohr Institute for its hospitality during the completion of this work. The work of G.A. is supported by STFC. The work of K.S. is funded by the Danish Natural Science Research Council.

References

[1] P. de Forcrand, *Simulating QCD at finite density*, *PoS* **LAT2009** (2009) 010 [arXiv:1005.0539] [SPIRES].

[2] M.A. Stephanov, *Random matrix model of QCD at finite density and the nature of the quenched limit*, *Phys. Rev. Lett.* **76** (1996) 4472 [hep-lat/9604003] [SPIRES].

[3] J.C. Osborn, *Universal results from an alternate random matrix model for QCD with a baryon chemical potential*, *Phys. Rev. Lett.* **93** (2004) 222001 [hep-th/0403131] [SPIRES].

[4] G. Akemann, J.C. Osborn, K. Splittorff and J.J.M. Verbaarschot, *Unquenched QCD Dirac operator spectra at nonzero baryon chemical potential*, *Nucl. Phys.* **B 712** (2005) 287 [hep-th/0411030] [SPIRES].

[5] T.D. . Cohen, *Functional integrals for QCD at nonzero chemical potential and zero density*, *Phys. Rev. Lett.* **91** (2003) 222001 [hep-ph/0307089] [SPIRES].

[6] J.C. Osborn, K. Splittorff and J.J.M. Verbaarschot, *Chiral symmetry breaking and the Dirac spectrum at nonzero chemical potential*, *Phys. Rev. Lett.* **94** (2005) 202001 [hep-th/0501210] [SPIRES].

JHEP08(2010)017

[7] J.C. Osborn, K. Splittorff and J.J.M. Verbaarschot, *Chiral condensate at nonzero chemical potential in the microscopic limit of QCD*, *Phys. Rev.* **D 78** (2008) 065029 [arXiv:0805.1303] [SPIRES].

[8] T. Banks and A. Casher, *Chiral symmetry breaking in confining theories*, *Nucl. Phys.* **B 169** (1980) 103 [SPIRES].

[9] Z. Fodor and S.D. Katz, *A new method to study lattice QCD at finite temperature and chemical potential*, *Phys. Lett.* **B 534** (2002) 87 [hep-lat/0104001] [SPIRES].

[10] Z. Fodor and S.D. Katz, *Lattice determination of the critical point of QCD at finite T and mu*, *JHEP* **03** (2002) 014 [hep-lat/0106002] [SPIRES].

[11] Z. Fodor and S.D. Katz, *Critical point of QCD at finite T and mu, lattice results for physical quark masses*, *JHEP* **04** (2004) 050 [hep-lat/0402006] [SPIRES].

[12] Z. Fodor, S.D. Katz and K.K. Szabo, *The QCD equation of state at nonzero densities: lattice result*, *Phys. Lett.* **B 568** (2003) 73 [hep-lat/0208078] [SPIRES].

[13] C.R. Allton et al., *The QCD thermal phase transition in the presence of a small chemical potential*, *Phys. Rev.* **D 66** (2002) 074507 [hep-lat/0204010] [SPIRES].

[14] C.R. Allton et al., *The equation of state for two flavor QCD at non-zero chemical potential*, *Phys. Rev.* **D 68** (2003) 014507 [hep-lat/0305007] [SPIRES].

[15] C.R. Allton et al., *Thermodynamics of two flavor QCD to sixth order in quark chemical potential*, *Phys. Rev.* **D 71** (2005) 054508 [hep-lat/0501030] [SPIRES].

[16] R.V. Gavai and S. Gupta, *Pressure and non-linear susceptibilities in QCD at finite chemical potentials*, *Phys. Rev.* **D 68** (2003) 034506 [hep-lat/0303013] [SPIRES].

[17] P. de Forcrand and O. Philipsen, *The QCD phase diagram for small densities from imaginary chemical potential*, *Nucl. Phys.* **B 642** (2002) 290 [hep-lat/0205016] [SPIRES].

[18] P. de Forcrand and O. Philipsen, *The QCD phase diagram for three degenerate flavors and small baryon density*, *Nucl. Phys.* **B 673** (2003) 170 [hep-lat/0307020] [SPIRES].

[19] P. de Forcrand and O. Philipsen, *The chiral critical line of $N_f = 2 + 1$ QCD at zero and non-zero baryon density*, *JHEP* **01** (2007) 077 [hep-lat/0607017] [SPIRES].

[20] P. de Forcrand and O. Philipsen, *Constraining the QCD phase diagram by tricritical lines at imaginary chemical potential*, arXiv:1004.3144 [SPIRES].

[21] M. D'Elia and M.-P. Lombardo, *Finite density QCD via imaginary chemical potential*, *Phys. Rev.* **D 67** (2003) 014505 [hep-lat/0209146] [SPIRES].

[22] M. D'Elia and F. Sanfilippo, *The order of the Roberge-Weiss endpoint (finite size transition) in QCD*, *Phys. Rev.* **D 80** (2009) 111501 [arXiv:0909.0254] [SPIRES].

[23] S. Kratochvila and P. de Forcrand, *The canonical approach to finite density QCD*, *PoS* **LAT 2005** (2006) 167 [hep-lat/0509143] [SPIRES].

[24] A. Alexandru, M. Faber, I. Horvath and K.-F. Liu, *Lattice QCD at finite density via a new canonical approach*, *Phys. Rev.* **D 72** (2005) 114513 [hep-lat/0507020] [SPIRES].

[25] S. Ejiri, *Canonical partition function and finite density phase transition in lattice QCD*, *Phys. Rev.* **D 78** (2008) 074507 [arXiv:0804.3227] [SPIRES].

[26] Z. Fodor, S.D. Katz and C. Schmidt, *The density of states method at non-zero chemical potential*, *JHEP* **03** (2007) 121 [hep-lat/0701022] [SPIRES].

JHEP08(2010)017

[27] K. Splittorff, *Lattice simulations of QCD with $\mu(B) \neq 0$ versus phase quenched QCD*, hep-lat/0505001 [SPIRES].

[28] K. Splittorff, *The sign problem in the ϵ-regime of QCD*, *PoS* **LAT 2006** (2006) 023 [hep-lat/0610072] [SPIRES].

[29] G. Parisi, *On complex probabilities*, *Phys. Lett.* **B 131** (1983) 393 [SPIRES].

[30] J.R. Klauder, *Stochastic quantization*, H. Mitter, C.B. Lang eds., in *Recent Developments in High-Energy Physics*, Springer-Verlag, Wien Austria (1983), pg. 351.

[31] J.R. Klauder, *A Langevin approach to fermion and quantum spin correlation functions*, J. Phys. **A 16** (1983) L317 [SPIRES].

[32] J.R. Klauder, *Coherent-state Langevin equations for canonical quantum systems with applications to the quantized Hall effect*, *Phys. Rev.* **A 29** (1984) 2036.

[33] G. Aarts, *Can stochastic quantization evade the sign problem? — the relativistic Bose gas at finite chemical potential*, *Phys. Rev. Lett.* **102** (2009) 131601 [arXiv:0810.2089] [SPIRES].

[34] G. Aarts, *Complex Langevin dynamics at finite chemical potential: mean field analysis in the relativistic Bose gas*, *JHEP* **05** (2009) 052 [arXiv:0902.4686] [SPIRES].

[35] G. Aarts and I.-O. Stamatescu, *Stochastic quantization at finite chemical potential*, *JHEP* **09** (2008) 018 [arXiv:0807.1597] [SPIRES].

[36] J.R. Klauder and W.P. Petersen, *Spectrum of certain nonselfadjoint operators and solutions of Langevin equations with complex drift*, *J. Stat. Phys.* **39** (1985) 53.

[37] F. Karsch and H.W. Wyld, *Complex Langevin simulation of the SU(3) spin model with nonzero chemical potential*, *Phys. Rev. Lett.* **55** (1985) 2242 [SPIRES].

[38] J. Ambjørn and S.K. Yang, *Numerical problems in applying the Langevin equation to complex effective actions*, *Phys. Lett.* **B 165** (1985) 140 [SPIRES].

[39] J. Ambjørn, M. Flensburg and C. Peterson, *The complex Langevin equation and Monte Carlo simulations of actions with static charges*, *Nucl. Phys.* **B 275** (1986) 375 [SPIRES].

[40] J. Flower, S.W. Otto and S. Callahan, *Complex Langevin equations and lattice Gauge theory*, *Phys. Rev.* **D 34** (1986) 598 [SPIRES].

[41] E.-M. Ilgenfritz, *Complex Langevin simulation of chiral symmetry restoration at finite baryonic density*, *Phys. Lett.* **B 181** (1986) 327 [SPIRES].

[42] P.H. Damgaard and H. Huffel, *Stochastic quantization*, *Phys. Rept.* **152** (1987) 227 [SPIRES].

[43] J. Berges and I.O. Stamatescu, *Simulating nonequilibrium quantum fields with stochastic quantization techniques*, *Phys. Rev. Lett.* **95** (2005) 202003 [hep-lat/0508030] [SPIRES].

[44] J. Berges, S. Borsányi, D. Sexty and I.O. Stamatescu, *Lattice simulations of real-time quantum fields*, *Phys. Rev.* **D 75** (2007) 045007 [hep-lat/0609058] [SPIRES].

[45] J. Berges and D. Sexty, *Real-time gauge theory simulations from stochastic quantization with optimized updating*, *Nucl. Phys.* **B 799** (2008) 306 [arXiv:0708.0779] [SPIRES].

[46] C. Pehlevan and G. Guralnik, *Complex Langevin equations and Schwinger-Dyson equations*, *Nucl. Phys.* **B 811** (2009) 519 [arXiv:0710.3756] [SPIRES].

[47] G. Guralnik and C. Pehlevan, *Effective potential for complex langevin equations*, *Nucl. Phys.* **B 822** (2009) 349 [arXiv:0902.1503] [SPIRES].

JHEP08(2010)017

[48] G. Aarts, F.A. James, E. Seiler and I.-O. Stamatescu, *Adaptive stepsize and instabilities in complex Langevin dynamics*, *Phys. Lett.* **B 687** (2010) 154 [arXiv:0912.0617] [SPIRES].

[49] G. Aarts, E. Seiler and I.-O. Stamatescu, *The complex Langevin method: when can it be trusted?*, *Phys. Rev.* **D 81** (2010) 054508 [arXiv:0912.3360] [SPIRES].

[50] G. Aarts and F.A. James, *On the convergence of complex Langevin dynamics: the three-dimensional XY model at finite chemical potential*, arXiv:1005.3468 [SPIRES].

[51] L. Ravagli and J.J.M. Verbaarschot, *QCD in one dimension at nonzero chemical potential*, *Phys. Rev.* **D 76** (2007) 054506 [arXiv:0704.1111] [SPIRES].

[52] P.E. Gibbs, *Understanding finite baryonic density simulations in lattice QCD*, PRINT-86-0389 (GLASGOW) [SPIRES].

[53] P.E. Gibbs, *The fermion propagator matrix in lattice QCD*, *Phys. Lett.* **B 172** (1986) 53 [SPIRES].

[54] N. Bilic and K. Demeterfi, *One-dimensional qcd with finite chemical potential*, *Phys. Lett.* **B 212** (1988) 83 [SPIRES].

[55] M.-P. Lombardo, *Finite density (might well be easier) at finite temperature*, *Nucl. Phys. Proc. Suppl.* **83** (2000) 375 [hep-lat/9908006] [SPIRES].

[56] M.P. Lombardo, K. Splittorff and J.J.M. Verbaarschot, *Distributions of the phase angle of the Fermion determinant in QCD*, *Phys. Rev.* **D 80** (2009) 054509 [arXiv:0904.2122] [SPIRES].

[57] J. Ambjørn, K.N. Anagnostopoulos, J. Nishimura and J.J.M. Verbaarschot, *The factorization method for systems with a complex action - a test in random matrix theory for finite density QCD -*, *JHEP* **10** (2002) 062 [hep-lat/0208025] [SPIRES].

[58] P. Hasenfratz and F. Karsch, *Chemical potential on the lattice*, *Phys. Lett.* **B 125** (1983) 308 [SPIRES].

[59] J.C. Osborn, K. Splittorff and J.J.M. Verbaarschot, *The sign problem is the solution*, hep-lat/0510118 [SPIRES].

[60] M.P. Lombardo, K. Splittorff and J.J.M. Verbaarschot, *The fluctuations of the quark number and of the chiral condensate*, *Phys. Rev.* **D 81** (2010) 045012 [arXiv:0910.5482] [SPIRES].

JHEP08(2010)017